Eur. Phys. J. B **2**, 341–345 (1998)

THE EUROPEAN PHYSICAL JOURNAL B

The effect of added salt on polyelectrolyte structure

M.J. Stevens[a] and S.J. Plimpton

P.O. Box 5800, MS 1111, Sandia National Laboratories, Albuquerque, NM 87185, USA

Received: 9 July 1997 / Revised: 3 November 1997 / Accepted: 30 November 1997

Abstract. We present results of molecular dynamics simulations of strong, flexible polyelectrolyte chains in solution with added salt. The effect of added salt on the polyelectrolyte chain structure is fully treated for the first time as a function of polymer density. Systems above and below the Manning condensation limit are studied. The chain structure is intimately tied to the ion density near the chain even for chains in the counterion condensation (CC) regime. The end-to-end distance is demonstrated to be a function of the inverse Debye screening length and the Bjerrum length. The ion density near the polymer chain depends on the amount of added salt, and above the condensation limit the chains significantly contract due to added salt.

PACS. 61.25.Hq Macromolecular and polymer solutions; polymers melts; swelling – 36.20.Ey Conformation (statistics and dynamics) – 87.15.He Molecular dynamics and conformational changes

1 Introduction

Polyelectrolytes are a very important class of polymers, because they are one set of water-soluble polymers. They include biopolymers such as DNA, RNA, and polysaccharides. Their water solubility makes polyelectrolytes an important class of synthetic, commercial polymers used for example, as the key water absorbing ingredient in disposable diapers. The addition of salt is a key means to alter structure and properties. Our understanding of polyelectrolyte structure is limited, and consequently, so is our understanding of polyelectrolyte system properties [1–5]. Recently, simulations have calculated the structure of strong, flexible polyelectrolytes in salt-free solution [3]. Here, we present results of polyelectrolyte simulations with added salt. In particular we examine the influence of the ionic distribution on the chain structure.

Our understanding of polyelectrolytes has been poor because of the difficulties these systems present to both experiment and theory. Direct measurements of the single chain structure, particularly at dilute concentrations have yet to be done. Recent molecular dynamics (MD) simulations of salt-free polyelectrolyte systems have overcome major theoretical difficulties [3,6]. The picture of polyelectrolyte structure [3,5] has been shown to be more complicated than the two early theories [7] predicted. Past theoretical works tended to neglect entropy, in part because they focused on DNA which is intrinsically very stiff. For stiff chains entropy is a small contribution to the free energy. In contrast, for flexible polyelectrolytes, treating entropy along with the Coulomb interactions is essential and has only been done properly in simulations [3,5]. More recently, self-consistent field theory [8] and PRISM [9] calculations also treat entropy and are promising.

One of the major theoretical difficulties is the calculation of the ionic density about the chain. Almost all calculations of chain structure use the Debye-Hückel (DH) approximation. Moreover, to date analytic calculations have been for fixed shapes (*e.g.* cylinders). This approximation is a linearization of the Poisson-Boltzmann (PB) equation, valid when the Coulomb interaction energy is much less than $k_{\mathrm{B}}T$. Yet, polyelectrolytes are highly charged and the Coulomb energies are often stronger than $k_{\mathrm{B}}T$. The PB equation [10–12] is a mean field approximation that neglects ion correlations, and is valid when typical counterion separations are larger than the Bjerrum length, $\lambda = e^2/\epsilon k_{\mathrm{B}}T$, where ϵ is the dielectric constant of the solution (water) and e is the electron charge.

By performing MD simulations, we can treat the fundamental polyelectrolyte problem without any of the above approximations. Previously, using MD one of us has successfully characterized strong, flexible polyelectrolytes in salt-free solution [3,6]. Experimental measurements of the osmotic pressure and the peak position in the interchain structure factor were reproduced by these simulations. Furthermore, it was shown that polyelectrolyte structure is fundamentally different from previous theoretical predictions. In particular, the chains contract below the overlap density, ρ^*. The chains are not fully extended or rodlike at dilute concentrations. For fully flexible chains and $\lambda/a \sim 1$ entropy is not dominated by the Coulomb interactions. While the end-to-end distance is much larger than for neutral chains, the dilute conformation exhibits significant bending at large length scales.

[a] e-mail: mjsteve@cs.sandia.gov

2 Simulation methods

In this article we treat systems with added salt by extending the methods of previous works. The fundamental model of polyelectrolytes in solution consists of N_p polymer chains of charged monomers, an equal number (N) of oppositely charged free monomers (counterions) and, optionally, additional salt ions (equal numbers of both positive and negative free particles). The neutral solvent in this model is treated as a continuous dielectric background. We perform two types of MD simulations. In one, labeled 'Coulomb', the counterions and salt ions are explicitly included. These simulations completely treat the fundamental model. In the other simulations, labeled 'Debye-Hückel' or DH, the solvent ions are not modeled explicitly, but implicitly included within the Yukawa potential between monomers of the chains. These simulations treat the simplified model that is usually treated theoretically. This approximation greatly reduces the computational effort. As we show, in some cases the DH simulations are warranted, and in others they are not.

In this work, all ions are monovalent. All the monomers are charged so that the average bond length b equals the charge separation a. The systems contains multiple polyelectrolyte chains. The various densities are denoted as follows: polymer density, ρ_p, the monomer density, $\rho_m = N\rho_p$, and the added salt density, ρ_s.

In the Coulomb simulations the salt ions are modeled the same as the counterions. The number of added salt ions ranges from 0 to $8N_c$, where N_c is the number of counterions which is typically 256 or 512. The salt ions oppositely charged to the monomers are identical to the counterions. All ions including the monomers interact via a purely repulsive Lennard-Jones (RLJ) potential with the cutoff at $r_c = 2^{1/6}\sigma$:

$$U_{LJ}(r) = \begin{cases} 4\epsilon\left[\left(\frac{\sigma}{r_c}\right)^{12} - \left(\frac{\sigma}{r_c}\right)^{6} + \frac{1}{4}\right]; & r \le r_c \\ 0; & r > r_c. \end{cases} \quad (1)$$

The Coulomb coupling strength is determined by the Bjerrum length. One set of simulations were performed for the same parameter set as in the earlier salt-free work, $\lambda = 0.83\sigma$ or $\xi \equiv \lambda/a = 0.75$ [3]. In order to study the effects of counterion condensation, we also performed simulations with $\lambda = 3.2\sigma > a$ ($\xi = 2.9$) which corresponds to a fully charged chain when mapped to sodium polystyrene sulfonate [3]. For these Coulomb simulations we used the particle-particle particle-mesh algorithm to calculate the long range Coulomb interactions [13,14]. This algorithm's computation time scales roughly as $M \log M$, where M is the number of charged particles. Such scaling is essential to perform these calculations as added salt increases the number of charged particles significantly. The simulations performed here involve up to 10 times the number of charged particles as for the corresponding salt-free simulations [3]. Even with the near linear computational scaling these simulations are at the edge of computational capability. The largest system had 4608 particles (all charged) and ran for 3×10^5 timesteps. Some systems of 4096 total particles ($N = 64$) were run for 8×10^5 timesteps.

We also performed simpler simulations using the DH interaction instead of the full Coulomb interaction [12]. In this case the monomer-monomer interaction is

$$u_{ij}(r) = k_B T \lambda \exp(-\kappa r)/r, \quad (2)$$

where $\kappa = \Lambda_s^{-1} = (4\pi\lambda(2\rho_s + \rho_c))^{1/2}$ is the inverse Debye length, ρ_c is the counterion density and ρ_s is the salt density. For these simulations there are no explicit counterions or coions as their screening of the monomer-monomer interaction is treated by the DH interaction. This greatly reduces the cost of the simulation and yields reasonable values of the end-to-end distance for the $\lambda = 0.83\sigma$ case, but fails for $\xi \gtrsim 1$ [15]. The bond and RLJ monomer-monomer potentials remain the same for these simulations.

The polymers are modeled as freely-jointed bead-spring chains. Chains with $N = 32$, 64 and 128 monomers are treated. The number of chains is usually 8 with some simulations of up to 32 chains. The attractive part of the bond potential is the standard FENE (finite extendable, nonlinear elastic) potential

$$U_{FENE}(r) = -1/2kR_0^2 \ln(1 - r^2/R_0^2), \quad (3)$$

with $k = 7\epsilon/\sigma^2$ used for the spring constant, and with $R_0 = 2\sigma$ used for the maximum extent [16]. The repulsive part of the bond potential is the above LJ interaction so that the total bond potential is

$$U_{bond}(r) = U_{ch}(r) + U_{LJ}(r) \quad (4)$$

which gives an average bond length of $b = 1.1\sigma$.

The temperature is maintained at $T = 1.2\epsilon$, using the Langevin thermostat with damping constant $\Gamma = 1\tau^{-1}$. The timestep is 0.015τ. The number of timesteps needed to equilibrate and obtain good statistics for $N = 32$, 64 and 128 was about 3×10^5, 8×10^5, and 3×10^6 respectively.

3 Results

The effect of added salt on the chain structure is shown in Figure 1. The time averaged end-to-end distance, R, is plotted semilog *versus* the inverse Debye length κ. We normalize R by the neutral scaling $1.57N^{0.588}$, where the prefactor is determined from the present data. By this scaling the large κ regime where the ionic screening becomes complete should and does overlap for all N. In terms of Debye screening the monomer-monomer repulsion should be completely screened near $\Lambda_s = a/2$. Our results show that R does not reach the neutral chain value until $\Lambda_s \simeq 0.25\sigma$ or $a/4$. A further increase of ρ_s has negligible effect. At low κ the deviation for the different N is a function of the Coulombic repulsion. In the zero monomer density limit and infinite chain limit, the scaling for salt-free chains should be $R \sim N$ [7]. However, the previous salt-free simulation work has found that this limit is not

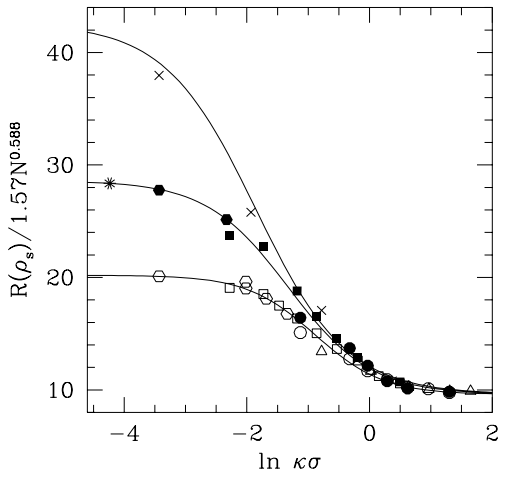

Fig. 1. The normalized end-to-end distance R as a function of the inverse Debye length. The open points are for $N = 32$; solid points $N = 64$; crosses $N = 128$. The different point shapes correspond to different monomer densities: $\rho_m\sigma^3 = 0.0001$ (hexagons), 0.001 (squares), 0.02 (triangles), 0.01 (circles). Also is included one point (asterisk) for $N = 64$ at $\rho_m\sigma^3 = 2 \times 10^{-5}$. The $N = 128$ data is for $\rho_m\sigma^3 = 0.01$. Error bars are about the size of the points.

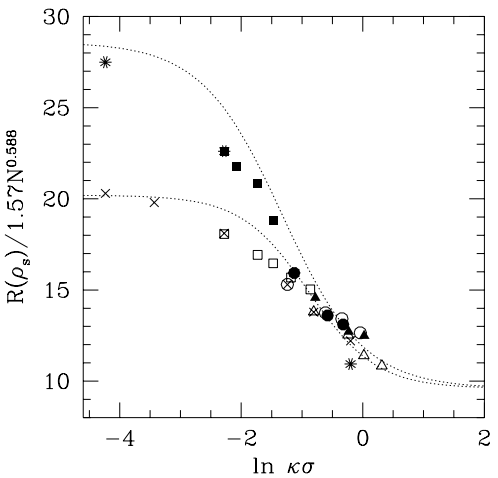

Fig. 2. The normalized end-to-end distance as a function of the inverse Debye length for full Coulomb simulations. Point types are the same as in Figure 1, except here the crosses are the salt-free $N = 32$ data and the asterisks are the salt free $N = 64$ data.

reached for chains (finite N) even at lowest realistic densities [3]. With added salt, we also observe a similar N-dependent saturation of R as κ decreases. This saturation is reminiscent of and clearly related to the saturation of R for salt-free systems as the density decreases [3,6].

Figure 1 shows that for a given N, R depends only on the value of κ, not on ρ_m. Different ρ_m will have different κ, but this just shifts the position of the points in the curve in Figure 1. The value of R is solely determined by κ. The densities studied here are mainly in the dilute regime at salt-free densities [3]. Since the chains shrink upon added salt, most of the data is well into the dilute regime. The value of R may depend on ρ_m, if ρ_m is above the overlap concentration. However, for $N = 128$ at $\rho_m = 0.01\sigma^{-3}$ and $\rho_s = 0.08\sigma^3$, we find $R = 25\sigma$. This case is well into the overlap regime (the overlap density is about $\rho_m^* = 0.001\sigma^{-3}$), and it fits (not shown) on curves in Figure 1.

We have fit the different N data in Figure 1 with a function of the form

$$y \equiv R/1.57(N/32)^{0.588} = \frac{A}{(\kappa\ell)^{2\alpha} + 1} + B, \qquad (5)$$

where A, B, ℓ and α are constants. This form was chosen just to satify the constraints for $\kappa \gg 0$ and for $\kappa \to 0$. At $\kappa = 0$, $y = A + B$ and the N-dependent saturation value is reached. For $\kappa \gg 0$ $y \to B = 9.6\sigma$, corresponding to the neutral value of y. Thus, α and ℓ are the only fit parameters. For $N = 32$, 64 and 128, the values of $\ell = 2.43$, 3.75 and 6.40 and $\alpha = 1.8$, 1.5 and 1.3, respectively.

At $\lambda/a = 0.75$, the results of the Coulomb simulation which treat the solvent ions explicitly are similar to, but smaller than the DH values. We show the data for the Coulomb simulations in Figure 2 with the same fitting curves as for Figure 1 (without the $N = 128$ line since there is no Coulomb data for this N). The Coulomb data exhibits the same lack of ρ_m dependence. In fact the data with added salt falls on the curves for the salt-free data. There is one small, but interesting exception. That is the point near $\ln \kappa\sigma = -0.2$ for $N = 64$ and $\rho_m = 0.064\sigma^{-3}$ and $\rho_s = 0$ which is below the other data points. This monomer density is above the overlap density. This suggests that the chain has become more contracted due to the repulsion of other chains.

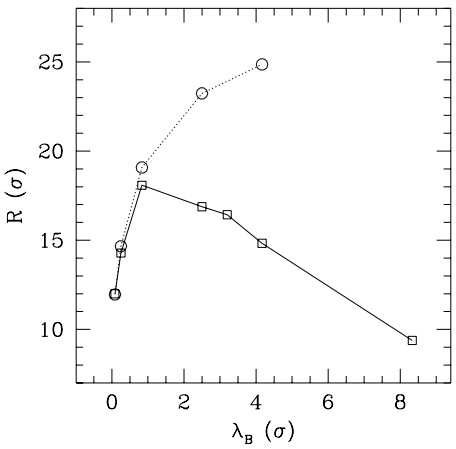

Fig. 3. Plot of end-to-end distance as a function of λ for DH simulations (◯) and Coulomb simulations (□). For these simulations $N = 32$ and $\rho_m = 0.001\sigma^{-3}$.

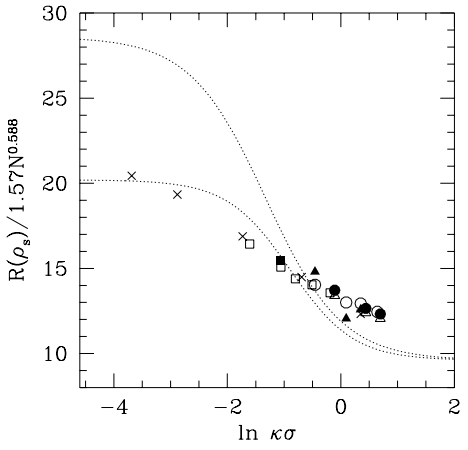

Fig. 4. The normalized end-to-end distance as a function of the inverse Debye length for full Coulomb simulations at $\lambda = 3.2\sigma$. Point types are the same as in Figure 2. In order to help comparison with the earlier data, we plot the same fitting curves to the DH data for $\lambda = 0.833\sigma$ as in the earlier figures.

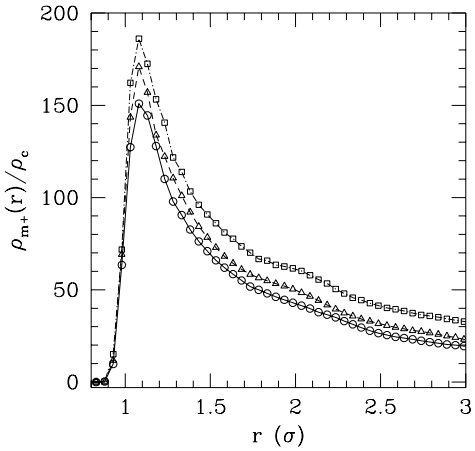

Fig. 5. Ratio of the positive ion number density about a monomer to the bulk counterion number density for $N = 32$ at $\rho_m = 0.001\sigma^{-3}$ and $\lambda = 3.2\sigma$ for $\rho_s/\rho_m = 0$ (◯), 1 (△), and 8 (□). This system is in the counterion condensation limit and has a dilute polymer concentration.

We now turn to results in the CC regime at $\lambda = 3.2\sigma$ corresponding to fully charged sodium polystyrene sulfonate [3]. In this regime the full Coulomb simulations are essential. To demonstrate this we present Figure 3 which shows the value of R at $\rho_m = 0.001\sigma^{-3}$ as a function of varying λ for the Coulomb and DH simulations. Increasing λ at fixed ρ_s and ρ_m not only yields stronger screening (larger κ), but also the prefactor in the pair potential (Eq. (2)) increases. If $\lambda/a \ll 1$, then the prefactor is much less than kT for all interactions, and there is not much to screen in the first place. On the other hand as λ/a approaches 1, the bare Coulomb interactions become strong and screening may be significant. From the figure, we see that for the DH simulations R is monotonically increasing. This implies that the increase in screening is not sufficient to offset the increase in the bare Coulomb strength [17]. Comparison with the full Coulomb simulations show that near $\lambda/a = 1$ the DH approximation breaks down. This occurs right where the Coulomb energy of next-nearest neighbors on the chain is about $1/2kT$ and no longer weak. The Manning approximation of renormalizing λ/a to 1 is also poor since it would yield a horizontal line in the figure, and the Coulomb data has R decreasing. These results are particularly relevant, since most fully charged polyelectrolytes are in the $\lambda/a > 1$ regime. We now examine this regime in more detail using full Coulomb simulations.

In Figure 4 we show the scaled plot of R for $\lambda = 3.2\sigma$. Comparison with Figure 2 shows that the larger λ has larger R for $\ln \kappa\sigma \geq -0.5$. At smaller κ the values of R for the Coulomb data at the two different λ become similar. Note that is partly an effect of plotting *versus* κ which is a function of λ. At the same ρ_m and ρ_s, the end-to-end distance is smaller for $\lambda = 3.2\sigma$ than for $\lambda = 0.83\sigma$ which is consistent with Figure 3. Since κ is a function of λ, the plot of R *versus* λ exhibits a different behavior. For the same values of κ, R tends to be larger for $\lambda = 3.2\sigma$ than for $\lambda = 0.83\sigma$. R as a function of κ clearly depends on the value of λ.

The structure of polyelectrolyte chains is determined by the ionic density of conterions and salt ions about the chains. We discuss the ionic densities for $\xi > 1$, where ions can become effectively trapped or 'condense' onto the chain. In Figure 5 we directly examine the ionic distributions. The figure shows the normalized radial ion number density, $\rho_{m+}(r)$, of all positive ions (*i.e.* counterion and positive salt) about a negatively charged monomer for $N = 32$, $\lambda = 3.2\sigma$ and $\rho_m = 0.001\sigma^{-3}$ at several salt densities. This distribution is calculated from the monomer-positive ion radial distribution function (rdf). The number density is calculated by multiplying the rdf by the average positive ion density. We then normalized by the counterion density.

There is a significant dependence on ρ_s at small r. The density is consistently higher for larger ρ_s. This contradicts the simple DH picture of a fixed ionic density near the chain [18], but exhibits a ρ_s dependence found in PB [19] and HNC solutions [20]. The difference in ρ_{m+} at small r is especially important, because this ionic density screens the monomer-monomer interactions. At $r = 3\sigma$, there is a 50% increase in the ion density for $\rho_s = 8\rho_m$ over $\rho_s = 0$. Thus, *within the volume of the chain the ion density increases as* ρ_s *increases.* The repulsion between monomers distant along the chain is increasingly screened by increasing ρ_s, and thus the chains contract even when counterion condensation occurs. These results are more consistent with solutions of the PB [19] and HNC equations [20] for charged cylinders. They contradict CC theory which claims that the ion condensation is dependent

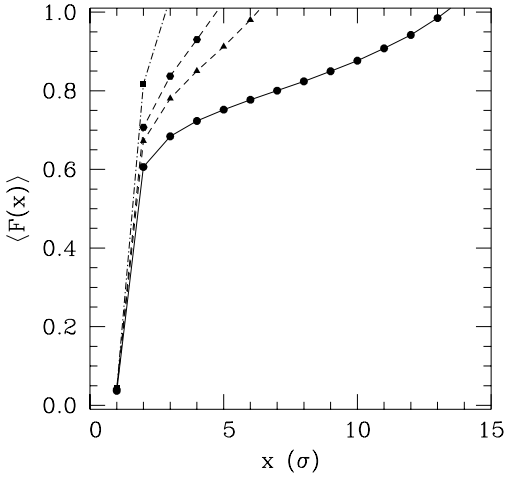

Fig. 6. Fractional number of the positive ions within x of a chain for the same systems as Figure 5. $\rho_s/\rho_m = 0$ (circle), 1 (triangle), 2 (hexagon) and 8 (square). The Manning condensation fraction for these systems is 0.65.

on salt concentration. For the flexible chains the Coulomb energy can be decreased by bending the chain and bringing more oppositely charged particles closer together. The system entropy increases since the chains access more conformations. The condensed ions also access the larger configuration space that the chains possess increasing their entropy. Thus, on both accounts the free energy improves.

The number of ions near a chain can be directly counted. We define the distance between an ion and the chain to be the minimum of the distances between the ion and each monomer in the chain. Using this metric, we can calculate the number of ions within a distance x to $x + \mathrm{d}x$ of the chain. Normalizing by N, we obtain the fractional number, $f(x)$. Integrating $f(x)$ gives the total fractional number of ions within a distance, x, which we define as $F(x)$. If each chain on average has N counterions within x_N of it, then $F(x_N) = 1$. In the case of added salt, since the counterions and positive salt ions are indistinguishable, we calculate F where an ion is either a counterion or a positive salt ion. Note that $F(x)$ can now be greater than one, and this will clearly happen for large enough x. Figure 6 shows $F(x)$ for the same systems as Figure 5. Because of steric repulsion, there are almost no ions within 1σ of the chains. Within 2σ there are a substantial number of ions. At $\rho_s = 0$, $F(2\sigma) = 0.60$ which is less than the Manning fraction for linear chains, $1/\xi = 0.65$. This ionic fraction at the chain as well as further from the chain varies substantially with salt density. In particular, with increasing ρ_s, $F(2\sigma)$ increases to about 0.82 at $\rho_s = 8\rho_m$. Furthermore, within less than 3σ, F reaches 1! This directly confirms that the ionic density increases significantly near the chains with increasing salt density.

The simulations presented here on polyelectrolytes with added salt have several important results. For the case with $\lambda/a < 1$, we find that the end-to-end distance for dilute concentrations depends on the value of κ and not ρ_s and ρ_m independently. This appears to remain true for different λ, but R as a function of κ depends also on λ. We directly demonstrated that for $\lambda/a > 1$ the DH model of polyelectrolytes breaks down even including the Manning approximation of setting $\lambda/a = 1$. Examining the ionic densities about a chain show that with increasing added salt the ionic density increases near the chain. This is consistent with minimizing both the Coulombic and entropy free energies.

This work was supported by the DOE under contract DE-AC04-94AL8500. Sandia is a multiprogram laboratory operated by Sandia Corp., a Lockheed Martin Company, for the DOE.

References

1. *Molecular Dynamics Simulations of Charged Polymer Chains From Dilute to Semidilute Concentrations*, edited by K. Schmitz, (American Chemical Society, D.C. Washington, 1994).
2. S. Förster, M. Schmidt, Adv. Polym. Sci. **120**, 51 (1995).
3. M. Stevens, K. Kremer, J. Chem. Phys. **103**, 1669 (1995).
4. J.-L. Barrat, J.-F. Joanny, Adv. Chem. Phys. **94**, 1 (1996).
5. U. Micka, K. Kremer, Phys. Rev. **E54**, 2653 (1996); Europhys. Lett. **38**, 279 (1997).
6. M. Stevens, K. Kremer, Macromol. **26**, 4717 (1993); Phys. Rev. Lett. **71**, 2228 (1993).
7. T. Odijk, J. Polym. Sci. Polym. Phys. Ed. **15**, 477 (1977); J. Skolnick, M. Fixman, Macromol. **10**, 944 (1977); J.-L. Barrat, J.-F. Joanny, Europhys. Lett. **3**, 343 (1993).
8. J. Donley, J. Rudnick, A.J. Liu, Macromol. **30**, 1188 (1997).
9. A. Yethiraj, Phys. Rev. Lett. **78**, 3789 (1997).
10. L. Guldbrand, B. Jönsson, H. Wennerström, P. Linse, J. Chem. Phys. **80**, 2221 (1984).
11. R. Kjellander, S. Marčelja, Chem. Phys. Lett. **112**, 49 (1984).
12. M. Stevens, M. Falk, M.O. Robbins, J. Chem. Phys. **104**, 5209 (1996).
13. R. Hockney, J. Eastwood, Computer Simulation using Particles (Adam Hilger, New York, 1988).
14. E.L. Pollock, J. Glosli, Comput. Phys. Commun. **95**, 93 (1996).
15. For salt-free systems, some quantities are not as accurately calculated in the DH approximation, see M. Stevens, K. Kremer, J. Phys. I France **6**, 1607 (1996).
16. B. Dünweg, K. Kremer, Phys. Rev. Lett. **66**, 2996 (1991).
17. For sufficiently large λ, the exponential screening dominates, but as in this case such large values tend to be unphysical.
18. G. Manning, Q. Rev. Biophys. **11**, 179 (1978).
19. M. Guéron, G. Weisbuch, Biopolym. **19**, 353 (1980).
20. R. Bacquet, P. Rossky, J. Phys. Chem. **88**, 2660 (1984).